No. 112/19, 60–68
ISSN 2657-6988 (online)
ISSN 2657-5841 (printed)
DOI: 10.26408/112.05

Submitted: 15.08.2019
Accepted: 25.11.2019
Published: 30.12.2019

ELASTIC CONSTANTS BY RESONANT ULTRASOUND SPECTROSCOPY – APPLICATION TO THERMOELECTRICS AND ALUMINUM ALLOYS

Benedikt Klobes

University of Applied Sciences, Bremerhaven, Laboratory of Nanotechnology,
An der Karlstadt 8, 27568 Bremerhaven, Germany,
e-mail: bklobes@hs-bremerhaven.de

Abstract: Resonant ultrasound spectroscopy is a non-destructive technique for determining the elastic constants of a material. In the context of thermoelectric materials, elastic constants can be used to investigate the speed of sound and, thus, the lattice thermal conductivity of a substance. For Mg_2Si-Mg_2Sn solid solutions, a possible connection between shear modulus and band convergence can be assumed in that way. Moreover, the rather low speed of sound in this system points towards a high contribution of optical phonons to thermal conductivity. Additionally, significant resonance frequency shifts are observed during natural aging of technical Al-Cu-Mg and Al-Mg-Si alloys, which are proposed to assist investigation of the early stages of clustering in the future.

Keywords: resonant ultrasound spectroscopy, elastic constants, thermoelectric materials, age hardening, aluminum alloys.

1. INTRODUCTION

Elastic constants are fundamental parameters of materials which characterize the elastic response of a solid to external forces. They can be used to assess possible structural applications and technical limitations of materials and, besides, are intimately linked to thermodynamic quantities such as specific heat and others such as the speed of sound. Determining elastic constants, particularly if the term is understood as components of the elastic tensor [Lovett 1990], is however a non-trivial task.

A modern, non destructive approach to determining elastic constants is resonant ultrasound spectroscopy [Maynard 1996]. It allows for extracting the full elastic tensor if single crystals are used and, anyhow, *the* elastic modulus C_{11} as well as *the* shear modulus C_{44} if polycrystalline, i.e. isotropic materials are used. In the following the method of resonant ultrasound spectroscopy is described in more detail and two timely applications are presented. Elasticity of thermoelectric

Mg_2Si-Mg_2Sn solid solutions is investigated based on results previously published in [Klobes et al. 2019]. Additionally, it is argued that resonant ultrasound spectroscopy may be a complimentary technique for investigating the early stages of precipitation in aluminum alloys.

2. RESONANT ULTRASOUND SPECTROSCOPY

Elastic constants of solids can be determined in different ways with resonant ultrasound spectroscopy (RUS) rather uniquely combining a non-destructive approach with (potential) access to the complete elastic tensor.

The schematic diagram of a basic experimental RUS setup is shown in Fig. 1. A sample of a usually known and well-defined shape is sandwiched between two piezoelectric transducers, which serve as an ultrasound emitter and transceiver, respectively. As even in the case of mechanical resonance, ultrasound is strongly damped by transmission through the sample, a lock-in amplifier [Meade 1983], which is also connected to the exciting function generator, is used to extract the transmitted signal. By determining the in- and out-of phase components, X and Y, resonance frequencies can be clearly observed. An experimental RUS spectrum of one of the thermoelectric samples discussed in section 3 is shown in Fig. 2 and highlights the unambiguousness of resonance frequencies.

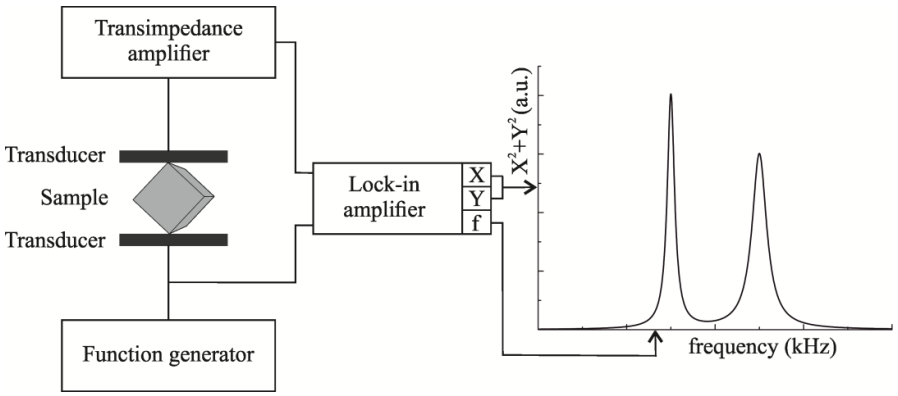

Fig. 1. Schematic measurement setup of resonant ultrasound spectroscopy. A sample is mounted between two piezoelectric transducers used as transmitter and receiver, respectively. A lock-in amplifier serves as the central element and determines whether a certain ultrasonic frequency is transmitted through the sample. Displaying in-phase and π/2-phase shifted components, X and Y, vs. frequency f yields the resonance spectrum

The calculation of mechanical resonance frequencies of a sample with volume *V* and free surface *S* is usually based on the Lagrangian formalism, *i.e.*, on the minimization of the Lagrangian

$$L = \int_V \left(\frac{1}{2} \sum_i \rho \omega^2 u_i^2 - \frac{1}{2} \sum_{i,j,k,l} C_{ijkl} \frac{\partial u_i}{\partial x_j} \frac{\partial u_k}{\partial x_l} \right) dV$$

where ρ is the mass density, ω is the angular frequency, u_i is the *i*th component of the displacement vector with respect to the coordinate system, and C_{ijkl} is the elastic tensor. The first and second term of the Lagrangian represent kinetic energy and the potential energy, respectively. Expanding the displacement vector in a complete set of functions $\{\theta_\gamma\}$, i.e. $u_i = \sum_\gamma a_{i\gamma} \theta_\gamma$, and calculating the stationary points of the Lagrangian with respect to the coefficients $a_{i\gamma}$, an eigenvalue equation is obtained which contains resonance frequencies and corresponding normal modes of the solid. A more detailed account of the theoretical background of RUS is beyond the scope of this manuscript (see Refs. [Migliori and Sarrao 1997] and [Zadler et al. 2004] for a more comprehensive introduction instead); it is, however, noteworthy that in the case of samples featuring a rectangular parallelepiped-shape comparatively simple solutions to the minimization problem can be derived. In any case, resonance frequencies can be calculated if sample dimensions, sample mass, elastic constants, and the crystallographic orientation with respect to the sample surfaces are known.

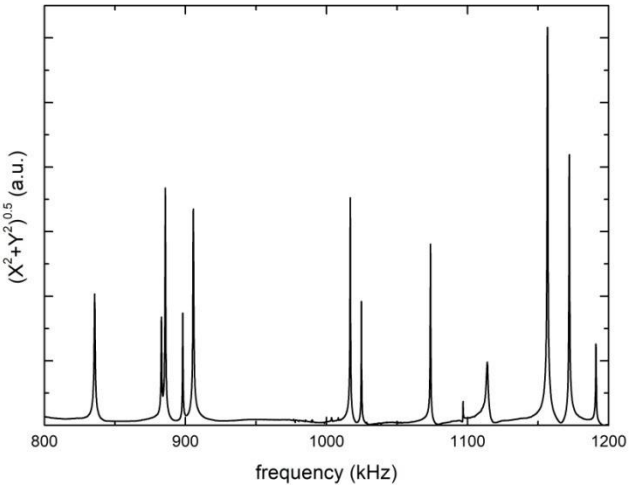

Fig. 2. Representative RUS spectrum. In most cases, resonance frequencies can be easily distinguished from background contributions

In contrast, determining elastic constants from experimentally observed resonance frequencies is an inverse problem with no unique solution. Thus, elastic constants are often fit using a non-linear least squares algorithm (for an actual implementation see [Le Rousseau, Watson and Freeman 2015]), in order to find an optimal match between calculated and observed resonance frequencies.

3. ELASTIC CONSTANTS OF MG_2SI-MG_2SN SOLID SOLUTIONS

Recovering waste heat of industrial or other processes is an essential measure for increasing energy efficiency. Among the different approaches for waste heat recovery, thermoelectric energy generation is particularly promising as it requires no moving parts [Goldsmid 2016].

Thermoelectric energy generation is routed in the diffusion of charge carriers due to temperature gradients. The thermoelectric figure-of-merit $ZT = \frac{S^2\sigma}{\kappa_e+\kappa_l}T$ of thermoelectric materials, where S is the Seebeck coefficient, σ is the electrical conductivity, κ_e and κ_l are the electronic and lattice parts of the thermal conductivity, and T is the temperature [Goldsmid 2016], illustrates that well performing thermoelectric materials need to exhibit conflicting transport properties.

A popular strategy in thermoelectric materials development and science is thus the reduction of thermal conductivity without decreasing the Seebeck coefficient or electrical conductivity. This can be achieved by introducing phonon scattering centers such as grain boundaries, guest atoms in empty crystallographic sites, or mass fluctuations, amongst others. The former two approaches eventually lead to nanocomposite materials with nanometer-sized grains [Liu et al. 2012] and rattling atoms in host-guest structures, e.g. skutterudites [Toberer, Zevalkink and Snyder 2011]; the latter one can be simply obtained in solid solution phases [Toberer, Zevalkink and Snyder 2011].

Solid solutions based on Mg_2Si and Mg_2Sn exhibit favorable ZT values competitive with the thermoelectric gold standard PbTe, not least due to low thermal conductivity, and are inexpensive, abundant and non-toxic, which in total renders this material system highly interesting for applications. Moreover, the high thermoelectric figure-of-merit found in $Mg_2Si_{1-x}Sn_x$ was associated with a convergence of electronic bands, which raises the question of potential band structure effects on elastic and vibrational properties. To some extent, this question was addressed in Ref. [Klobes et al. 2019] and the results published in the aforementioned reference are summarized in the following.

Thus, elastic constants of polycrystalline $Mg_2Si_{1-x}Sn_x$ were investigated at room temperature using RUS and the results for C_{11} and C_{44}, which can be associated with Young's modulus and shear modulus, are summarized in Tab. 1.

Additionally, the longitudinal, v_L, transversal, v_T, and average speed of sound, v_S, were calculated, which are also shown in Tab. 1. The calculations were carried out using $v_{L,T} = \sqrt{C_{11,44/\rho}}$ and $3v_S^{-3} = v_L^{-3} + 2v_T^{-3}$ [Anderson 1963], where ρ is the sample mass density. Both elastic constants as well as the different speed of sounds decrease with increasing Sn content, which is in line with the higher elastic constants of Mg_2Si compared to those of Mg_2Sn. At the same time, the decrease of the shear modulus is much more pronounced than expected, which might indicate an actual effect of band convergence close to $Mg_2Si_{0.4}Sn_{0.6}$.

Table 1. Elastic constants C_{11} and C_{44} as well as calculated longitudinal, v_L, transversal, v_T, and average speed of sound, v_S. of some Mg_2Si-Mg_2Sn solid solutions. Additions of Sb and Bi tune electrical properties and negligibly affect vibrational properties. This data was previously published in a different form in Ref. [Klobes et al. 2019]

Sample	C_{11} (GPa)	C_{44} (GPa)	v_L (m/s)	v_T (m/s)	v_S (m/s)
$Mg_2Si_{0.79}Sn_{0.2}Sb_{0.01}$	112(2)	44.5(5)	6990(60)	4404(25)	4850(70)
$Mg_2Si_{0.49}Sn_{0.5}Bi_{0.01}$	95(1)	36.3(0.5)	5910(30)	3655(25)	4030(60)
$Mg_2Si_{0.44}Sn_{0.55}Bi_{0.01}$	94(1)	33.7(0.5)	5870(30)	3514(26)	3890(60)
$Mg_2Si_{0.39}Sn_{0.6}Bi_{0.01}$	86(2)	29(1)	5600(70)	3250(60)	3610(50)

With respect to thermal conductivity, the average speed of sound can be used to estimate the lattice contribution to thermal conductivity, κ_l, within a simple Callaway model using $\kappa_l = \frac{1}{3} C v_S^2 \tau$ [Callaway 1959], where C is the specific heat and τ is the phonon relaxation time. Such calculations (for details cf. [Klobes et al. 2019]) yield lattice thermal conductivities of around 1.5 W/m/K which is only about 60% of experimentally determined values [Dasgupta et al. 2014]. As the Callaway model takes into account solely acoustic phonons, it is possible to conclude that optical phonons play a significant role for thermal conductivity in this system.

4. RESONANCE SHIFTS DURING AGING OF ALUMINUM ALLOYS

Aluminum alloys have been used as structural materials for more than a century and, despite increasing competition with, for example, composite materials, continue to be used in weight critical contexts such as in aircraft construction. Particularly in the latter case, age hardenable aluminum alloys are used, which obtain their high strength characteristics by means of age hardening. Usually,

a supersaturated solid solution of the alloy is quenched and subsequently aged at potentially elevated temperatures in order to facilitate precipitate formation in the system [Anderson, Weritz and Kaufman 2018]. Depending on the aluminum alloy system, different metastable phases develop which hinder dislocation movement and, thus, harden the material.

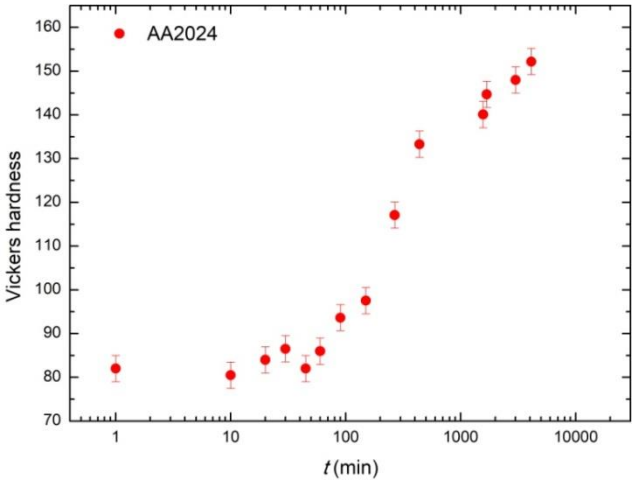

Fig. 3. Vickers hardness of an aluminum alloy AA2024 during natural aging. Each point represents the average of at least 6 individual measurements/indents. This data has been previously published in Ref. [Klobes, Maier and Staab 2011]

In the aerospace sector, age hardenable Al-Cu-Mg (belonging to the AA2000 designation) and Al-Mg-Si (the AA6000 designation) alloys are often applied. Al-Cu-Mg alloys are usually stored at room temperature (so called natural aging) in order to produce high strength, whereas Al-Mg-Si alloys are aged at elevated temperatures at around 180°C (so-called artificial aging). Fig. 3 exemplifies the impact of age hardening on aluminum alloys and shows a Vickers hardness measurement during natural aging after quenching the Al-Cu-Mg sample from about 560°C to room temperature.

Despite their long history, aluminum alloys are still intensively investigated due to arguably two reasons: Firstly, precipitation sequences have turned out to be more complex than expected [Yan 2014] and, secondly, the investigation of the very early stages of precipitation and solute cluster formation is still challenging or hardly possible. The size of solute clusters, which can contain only very few atoms, renders their detection and description very difficult (and at the cost of intensive sample preparation which likely alters the microstructure) or even impossible. Additionally, aluminum alloys containing Mg and/or Si as alloying elements suffer from the vanishing contrast between those neighbors in the periodic table, i.e. the small difference between Mg, Al, and Si in terms of atomic number. Eventually,

discriminating between Mg, Al, and Si contributions in such alloys can also be very difficult if probes such as photons or electrons are used. However, in recent years, some progress has been made using positron annihilation spectroscopy [Banhart et al. 2010; Klobes, Maier and Staab 2011], x-ray absorption spectroscopy [Klobes, Staab and Dudzik 2008; Petschke et al. 2018], and small angle scattering techniques [Ivanov, Deschamps and De Geuser 2017].

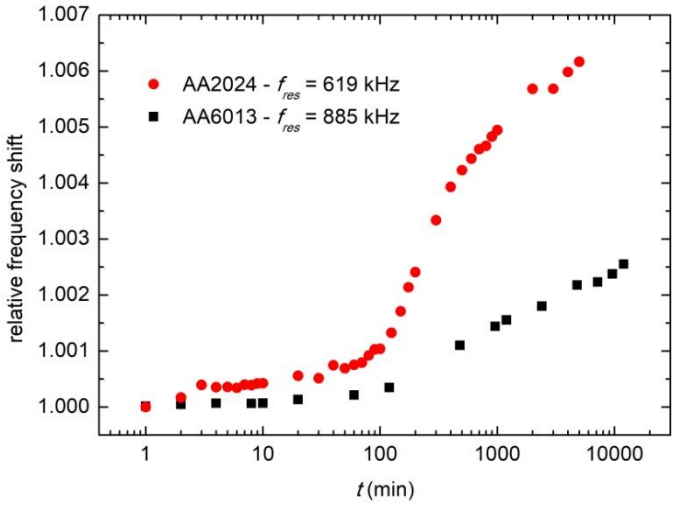

Fig. 4. Relative frequency shift of an arbitrarily selected, yet representative resonance frequency measured for an AA2024 and AA6013 sample. Error bars are smaller than the symbol

Within this context, RUS is proposed as a complimentary technique for the investigation of early stages of precipitation and cluster formation in aluminum alloys. Fig. 4 shows the relative frequency change of a specific (yet representative) resonance frequency of two AA2024 and AA6013 samples. During natural aging, i.e. room temperature storage, and continuous measurement the selected resonance frequency shifts towards higher values. Considering the hardness increase during aging, this frequency increase is somewhat expected as it reflects the increase of elastic constants. For the Al-Cu-Mg alloy AA2024 however, there is a significant increase during the very first three minutes of aging which is not reflected by the hardness measurements. Notably, this increase is not due to systematic noise and is not caused by outliers as it can be repeatedly measured for similarly prepared samples. Although the increase of resonance frequency does not facilitate a direct microscopic interpretation, it clearly shows that the first three minutes constitute a separate aging state from an elasticity perspective. For comparison, the strong increase starting at about 100 min is clearly reflected by the hardness increase in Fig. 3. In the future, such measurements may be complemented with ab-initio

calculations of the elastic constants due to different clusters, in order to determine exactly which kind of clusters give rise to such an increase.

5. CONCLUSIONS

Resonant ultrasound spectroscopy has been applied to investigate thermoelectric Mg_2Si-Mg_2Sn solid solutions and aluminum alloys AA2024 and AA6013.

It has been found that both elastic constants as well as the speed of sound decrease with increasing Sn content. The determined speeds of sound yield rather low values for lattice thermal conductivities in a Callaway model, which points towards a significant contribution of optical phonons to lattice thermal conductivity.

In age-hardenable aluminum alloys, an increase of resonance frequencies can be observed during natural aging, which is in line with hardness increase during that process. In Al-Cu-Mg based AA2024, a first aging stage in the very first minutes of aging can be observed. This may be utilized as a complimentary technique in future aging studies.

6. ACKNOWLEDGEMENTS

J. de Boor (German Aerospace Center, Germany), R.P. Hermann (Oak Ridge National Laboratory, USA), M.Y. Hu and A. Alatas (both Advanced Photon Source, USA) are thanked for a fruitful collaboration with respect to thermoelectrics. Financial support by the University of Applied Sciences, Bremerhaven for building a RUS spectrometer is acknowledged.

REFERENCES

Anderson, O.L., 1963, *A Simplified Method for Calculating the Debye Temperature from Elastic Constants*, Journal of Physics and Chemistry of Solids, vol. 24, no. 7, pp. 909–917.

Anderson, K., Weritz, J., Kaufman, J.G. (ed.), 2018, *ASM Handbook, Aluminum Science and Technology*, ASM International, Novelty.

Banhart, J., Chang, C.S.T., Liang, Z., Wanderka, N., Lay, M.D.H., Hill, A.J., 2010, *Natural Aging in Al-Mg-Si Alloys – A Process of Unexpected Complexity*, Advanced Engineering Materials, vol. 12, no. 7, pp. 559–571.

Callaway, J., 1959, *Model for Lattice Thermal Conductivity at Low Temperatures*, Physical Review, vol. 113, no. 4.

Dasgupta, T., Stiewe, C., de Boor, J., Müller, E., 2014, *Influence of Power Factor Enhancement on the Thermoelectric Figure of Merit in Mg2Si0.4Sn0.6 Based Materials*, Physica Status Solidi A, vol. 211, no. 6, pp. 1250–1254.

Goldsmid, H.J., 2016, *Introduction to Thermoelectricity*, Springer-Verlag, Berlin Heidelberg, Germany.

Ivanov, R., Deschamps, A., De Geuser, F., 2017, *A Combined Characterization of Clusters in Naturally Aged Al–Cu–(Li, Mg) Alloys Using Small-angle Neutron and X-ray Scattering and Atom Probe Tomography*, Journal of Applied Crystallography, vol. 50, pp. 1725–1734.

Klobes, B, de Boor, J., Alatas, A., Hu, M.Y., Simon, R.E., Hermann, R.P., 2019, *Lattice Dynamics and Elasticity in Thermoelectric Mg2Si1−xSnx*, Physical Review Materials, vol. 3, 025404.

Klobes, B., Maier, K., Staab, T.E.M., 2011, *Natural Aging of Al–Cu–Mg Revisited from a Local Perspective*, Materials Science and Engineering A, vol. 528, pp. 3253–3260.

Klobes, B., Staab, T.E.M., Dudzik, E., 2008, *Early Stages of Decomposition in Al Alloys Investigated by X-ray Absorption*, Physica Status Solidi RRL, vol. 2, no. 4, pp. 182–184.

Le Rousseau, J.H.L., Watson, L., Freeman, P., 2015, *PALab Resonant Ultrasound Spectroscopy*, July 2019, https://github.com/PALab/RUS.

Liu, W., Yan, X., Chen, G., Ren, Z., 2012, *Recent Advances in Thermoelectric Nanocomposites*, Nano Energy, vol. 1, no. 1, pp. 42–56.

Lovett, D.R., 1990, *Tensor Properties of Crystal*, Adam Hilger, Bristol and New York, USA.

Maynard, J., 1996, *Resonant Ultrasound Spectroscopy*, Physics Today, vol. 49, no. 1, pp. 26–31.

Meade, M.L., 1983, *Lock-in Amplifiers: Principles and Applications*, Peter Peregrinus Ltd., London, England.

Migliori, A., Sarrao, J.L., 1997, *Resonant Ultrasound Spectroscopy: Applications to Physics, Materials Measurements, and Nondestructive Evaluation: Applications to Physics, Material Measurements and Nondestructive Evaluation*, John Wiley & Sons, New Jersey, USA.

Petschke, D., Lotter, F., Bläss, E., Staab, T.E.M., 2018, *Time-resolved X-ray Absorption Spectroscopy on Al–Cu Alloys – from Solute Copper to Stable Precipitates*, Journal of Applied Crystallography, vol. 51, no. 5, pp. 1339–1351.

Toberer, E.S., Zevalkink, A., Snyder, G.J., 2011, *Phonon Engineering through Crystal Chemistry*, Journal of Materials Chemistry, vol. 21, pp. 15 843–15 852.

Yan, Y., 2014, *Investigation of the Negative and Positive Effect of Natural Aging on Artificial Aging Response in Al-Mg-Si Alloys*, PhD-Thesis, Technische Universität Berlin, Germany.

Zadler, B.J., Le Rousseau, J.H.L., Scales, J.A., Smith, M.L., 2004, *Resonant Ultrasound Spectroscopy: Theory and Application*, Geophysical Journal International, vol. 156, no. 1, pp. 154–169.